Aerosol-Assisted CVD As The Economically Method to Deposit The Solar Cell, An Overview of The Electrical and Structural Properties

Nurfadzilah Ahmad[1], Habibah Zulkefle[2], Puteri Sarah Mohamad Saad[2], Sivaraju S. S[3], Nurdiyana Borhan[4], Wan Abd Al-Qadr Imad Wan Mohtar[5]

[1]Solar Research Institute (SRI), Universiti Teknologi MARA (UiTM) Shah Alam, Selangor, [2]School of Electrical Engineering, College of Engineering, Universiti Teknologi MARA (UiTM) Shah Alam, Selangor, [3]RVS College of Engineering and Technology, Coimbatore, Tamil Nadu, India, [4]Davex (Malaysia) Sdn. Bhd., Subang Jaya, Selangor, [5]Functional Omics and Bioprocess Development Laboratory, Institute of Biological Sciences, Faculty of Science, Universiti Malaya, 50603, Kuala Lumpur, Malaysia

Abstract

In the modern era, it is very crucial to utilize the sustainable energy that is abundant in nature especially the solar energy. Due to this reason the research to develop an economically solar cell has been extensively studied. Aerosol-Assisted CVD, an economically developed method to produce the carbon solar call has proven its ability in this area to produce the solar cell. Five samples of pure a-C and nitrogen doped a-C:N were produced, with deposition temperatures ranging from 400°C to 600°C. The current-voltage solar simulator characterization yielded an ohmic contact. Higher conductivity at a-C:N, x10-2 Scm-1 is attributable to a decrease in defects caused by the decrease in spin density gap with nitrogen addition. AFM measurements of structural characteristics at high temperatures reveal an even smoother image as the intense carbon ion bombardment at the thin film's surface increases.

Keywords: Pure a-C, Nitrogen Doped a-C N, Structural Properties, Electrical Properties.

Introduction

Carbon material has recently piqued the interest of semiconductor researchers due to its appealing features resulting from the tunable ratio of sp2 and sp3 carbon bonding ratios. One of the carbon branches, amorphous carbon (a-C), is stated to feature a mixture of sp2, sp3, and even sp1 carbon sites, allowing the a-C's properties to be tweaked as required (Tan et al., 2008). The a-C material is semiconducting, allowing it to take dopants (Podder et al., 2005), and it has a large band gap ranging from 0.0 eV to 5.5 Ev (Mominuzzaman et al., 2006). The a-C deposition parameter is also suitable with a low-cost glass substrate, as manufacturing temperatures can be as low as 350oC.

The low-cost chemical vapour deposition (CVD) technology was also used in the a-C production. However, several limitations of adopting the CVD approach include the lack of a suitable volatile precursor and the difficulty in controlling the stoichiometry of the deposition (Hou & Choy, 2006). To address these issues, the conventional CVD technique was modified into aerosol-assisted CVD (AACVD), which uses aerosol droplets to transport the precursor with the help of a carrier gas.We studied the use of AACVD to create the a-C, as well as employing the same approach to dope the a-C into an n-type a-C in this work. The dopant was nitrogen gas, N2, and a-C:N was generated. The photosensitivity of a-C:N is up to 6.2 eV, photoluminescence is up to 4.5 eV, it has a high resistivity, and it has a low dielectric constant (Nitta et al., 2003). Hou et al (2005); Kim et al (2007); Yang et al (2006) proposed the formation of nitrogen-containing carbon from several precursors, such as acetonitrile, pyrole, or polyacrylonitrile. At room temperature, the electrical and structural properties of both conditions were examined using the Bukoh Keiki CEP2000 solar simulator system and the Park System XE-100 atomic force microscope (AFM).

Experimental Procedures

Aerosol-assisted CVD (AACVD) was used to create the a-C and a-C:N utilising camphor oil ($C_{10}H_{16}O$) as a precursor. The AACVD method combines the use of a normal CVD system and the spray pyrolysis method with the help of a carrier gas. The carrier gas for the pure a-C was argon gas, which is an inert gas, whereas for the N doped a-C:N, nitrogen gas was chosen as the dopant gas, which simultaneously worked as the carrier gas. The carrier gas's primary function is to transport the camphor oil in gaseous form from the aerosol phase of the CVD to the heated substrate. To convert the liquid form of the precursor into the gaseous form, it was first heated to its vaporisation temperature (180oC). The temperature of deposition at furnace two was changed from 400oC to 600oC, with 5 samples each for a-C and a-C:N. The surface profiler DEKTAK VEECO 150 was used to measure the thickness of the samples, which ranged from 30nm to 70nm. The CVD system's furnace one was set to 200oC during the deposition process to aid in the atomization of the camphor oil. The deposition lasted 30 minutes. Bukoh Keiki CEP2000 solar simulator system at room temperature and Park System XE-100 atomic force microscope (AFM) were used to characterise the electrical and structural properties of deposited a-C and a-C: N thin films.

Results and Discussion
Electrical Properties

The electrical characteristics were investigated using the solar simulator system, and an ohmic graph was generated for both pure a-C and a-C:N, as shown in fig. 1. The supply voltage was set between -5 and 5 V. According to figures. 1 (a) and (b), pure a-C has a somewhat lower current value than a-C:N. The counter electrode was made of gold (Au) and had a thickness of 60nm. The current obtained for pure a-C was x10-7 A, but the current obtained for a-C: N when nitrogen was utilised as the dopant/carrier gas was 10-6 A. Both a-C and a-C:N were deposited on a glass substrate at five different temperatures (400oC, 450oC, 500oC, 550oC, and 600oC). The maximum slope of the ohmic graph was obtained at sample 600oC, and the slopes decrease as the deposition temperature rises. The greater the slope, the lower the resistance value. The resistivity (ρ) and conductivity (σ) values were estimated from the resistance value using equations (1) and (2), where R is the resistance acquired from the I-V curve, w is the electrode width, t is the thickness of the a-C thin film, and L is the electrode length.

$$\rho = \left(\frac{V}{I}\right)\left(\frac{wt}{L}\right) \quad \text{in unit } \Omega.\text{cm} \qquad (1)$$

$$\sigma = \frac{1}{\rho} \qquad \text{in unit S.cm}^{-1} \qquad (2)$$

The conductivity () of pure a-C was computed, and the maximum conductivity was 9.4×10^{-2} Scm-1 at 600oC, followed by 7.1×10^{-3} Scm-1 at 550oC, 1.9×10^{-4} Scm-1 at 500oC, 2.2×10^{-4} Scm-1 at 450oC, and 1.8×10^{-4} Scm-1 at 400oC. In contrast, conductivity increases with temperature in a-C:N, reaching 3.9×10^{-2} Scm-1 at 600oC, followed by 9.1×10^{-3} Scm-1 at 550oC, 2.2×10^{-3} Scm-1 at 500oC, 1.9×10^{-3} Scm-1 at 450oC, and 4.7×10^{-4} Scm-1 at 400oC. The electrical properties of thin films can be produced theoretically by changing the density of crystal defects such as the vacancy, grain boundary, and film surface, which can then be directly related to the carrier concentration and mobility of the electron at different thicknesses (Huang & Meng, 2007).

The samples deposited using nitrogen gas as the dopant/carrier gas have higher conductivity because nitrogen gas as the dopant gas for a-C can modify the conductivity of pure a-C from p-type to n-type. Because the spin density gap decreases with nitrogen addition, effective doping is said to reduce defects (Rusop et al., 2006). Aside from that, nitrogen addition has been shown to reduce compressive stress in films and increase conductivity (Liu et al., 2008). Furthermore, as previously noted, the modest rise in electrical conductivity is related to the removal of structural defects and restoration of structural order. As a result, the greater conductivity of nitrogen doped a-C:N can be attributed to this.

Increasing the deposition temperature results in a larger thickness value (as proven by surface profiler measurements). The importance of carrier concentration and mobility in conductivity fluctuation has been reported (Alibart et al., 2008). As the thickness increases, so will the carrier concentration and mobility (Huang & Meng, 2007). Aside from that, the existence of * (sp2 graphitic bonding) and * (sp2 and sp3 diamond bonding) contributes to a-C conductivity. The intensity of the * region increases with temperature, indicating the encouragement of sp2 bonding due to an increase in graphitic order (Endrino et al., 2009). The a-C and a-C:N materials have sp2 (graphitic) carbon bonding, and the ratio can be changed based on the deposition conditions, such as the deposition temperature (Zhu et al., 2009). The conductivity was believed to rise as the temperature rose. The increased conductivity of a-C and a-C:N films at higher temperatures (600oC) was due to the complete separation of the precursor atom and the development of more sp2 carbon bonding sites. More sp2 carbon bonding sites resulted in an increase in localised hopping states (Pradhan & Sharon, 2007). At lower temperatures, the a-C is credited to have a larger sp3 carbon bonding ratio, which explains the reduced conductivity.
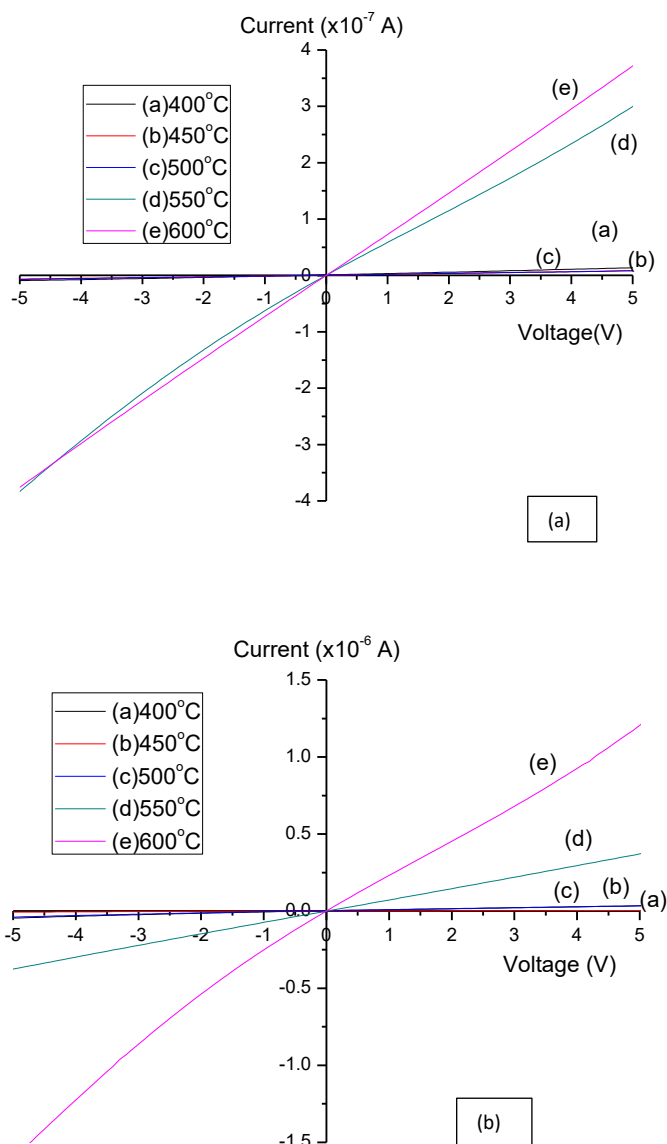
Fig.1. Current-voltage graph of (a) pure a-C and (b) nitrogen dope a-C:N at different deposition temperature

Structural Properties

Figures 2 and 3 show 3D pictures of pure a-C and nitrogen doped a-C:N obtained using Atomic Force Microscopy (AFM). Figure 2 shows irregular structures of pure a-C, with just a growth of a "island" structure at 400oC, but as the temperature rises, the structure becomes more even. There are some aggregation spots in the sample at 400oC, 450oC, and 500oC, which could be caused by poor carbon atom dispersion. In comparison to the other samples, the growth of a-C began to develop smoothly between 550oC and 600oC.

The AFM average roughness was calculated over a 30m x 30m region, and the roughness was not significantly affected by the deposition temperature. Within the scanning area, the sample has an average roughness of 0.361nm at 400oC, increasing to 1.080nm, 2.147nm, 8.219nm, and 0.391nm as the deposition temperature increases. However, for samples 400oC and 600oC, we can clearly see that the tiny value was caused by distinct factors, where at

400oC the small roughness value was caused by inappropriate carbon atom growth, and at 600oC the sample is smooth, therefore the roughness is minimal. The surface migration of the a-C particle is claimed to be accelerated for sample 550oC, resulting in the particle combining and creating the giant particle as compared to the lower deposition temperature (Valentini et al., 2001). On the other hand, as the temperature rises to 600oC, the sample becomes smoother, which could be attributed to an increase in the energetic carbon ion bombardment at the thin film's surface (Park & Hong, 2008).
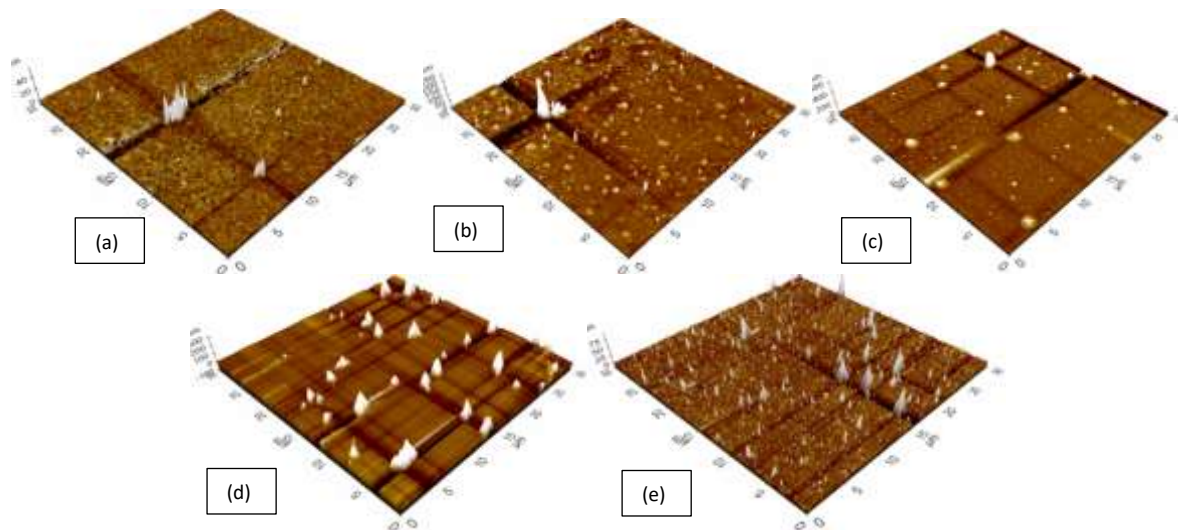
Fig.2. AFM images of pure a-C at different temperature
(a) 400°C (b) 450°C (c) 500°C (d) 550°C (e) 600°C

Nitrogen doped a-C:N exhibits consistent AFM pictures at 500oC, 550oC, and 600oC, whereas aggregation is observed at 400oC and 450oC. There was a carbon patch on the surface of both samples, and at 450oC, only a carbon 'tower' can be observed in the centre of the area, with no sign of carbon development in the surrounding area, highlighting the improper growth of carbon at the sample. The average roughness revealed was relatively minor, ranging from 0.00 nm to 1.463 nm, and was not affected by the deposition temperature. Figures 3(a) and (b) show an uneven dispersion of carbon particles, but as temperature increases, the structural properties of the a-C:N improve, indicating that lower temperatures were not suited for a-C:N growth. Aside from that, at the same deposition temperature, a-C:N has a superior structure than pure a-C. Small roughness suggests lower grain boundaries, which can be linked to the particle's proclivity to crystallise (Hagouel, 2005). The acquired roughness value was close to that reported by (Miyajima et al., 2005).

Overall, the findings indicate a link between deposition temperature and nitrogen doping in the growth of a-C and a-C:N. With increasing deposition temperature, a transition from a "island" structure to smaller particle and more uniform thin films with nitrogen presence occurs.
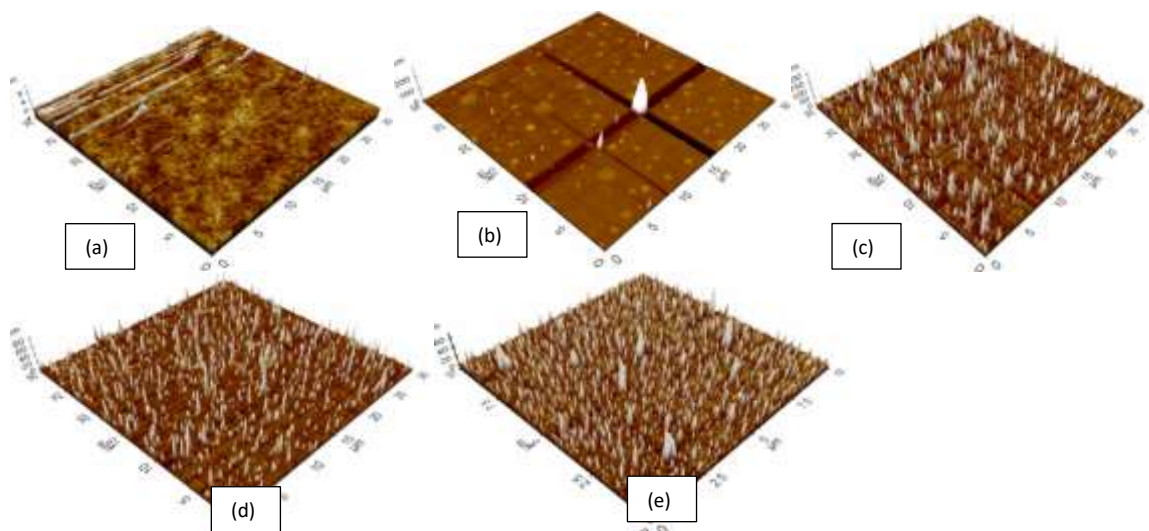
Fig.3. AFM images of nitrogen doped a-C:N at different temperature
(a) 400°C (b) 450°C (c) 500°C (d) 550°C (e) 600°C

Conclusion

Finally, a-C and a-C:N thin films were produced using the Aerosol-assisted CVD approach from the natural precursor camphor oil. The current-voltage solar simulator characterization yielded an ohmic contact with gold (Au) as the counter electrode. Higher conductivity at a-C:N results from a reduction in defects when the spin density gap decreases with nitrogen addition. Furthermore, the nitrogen addition reduces the compressive stress of the films, resulting in better conductivity. The roughness value of the AFM images varies depending on the deposition temperature of the pure a-C and the nitrogen doped a-C:N. Because of the more intense carbon ion bombardment at the thin film's surface at high temperatures, the AFM clarifies an even smoother image.

Contributions

The development of low-cost methods for manufacturing solar cells provides various benefits that can have a substantial impact on the solar business and renewable energy adoption. The primary advantage is affordability as the production costs are lower, solar cells are more affordable, making them available to a wider section of the population. This has the potential to expedite the adoption of solar energy in both industrialised and developing countries

Acknowledgements

References

Alibart, F., Durand Drouhin, O., Lejeune, M., Benlahsen, M., Rodil, S. E., & Camps, E. (2008). Evolution of the opto-electronic properties of amorphous carbon films as a function of nitrogen incorporation. *Diamond and Related Materials*, *17*(6), 925–930. https://doi.org/10.1016/J.DIAMOND.2008.01.080

Endrino, J. L., Horwat, D., Anders, A., Andersson, J., & Gago, R. (2009). Impact of Annealing on the Conductivity of Amorphous Carbon Films Incorporating Copper and Gold Nanoparticles Deposited by Pulsed Dual Cathodic Arc. *Plasma Processes and Polymers*, *6*(S1), S438–S443. https://doi.org/10.1002/PPAP.200931003

Hagouel, P. (2005). Semiconductor material and device characterization [Book Review]. *IEEE Circuits and Devices Magazine*, *15*(3), 36–36. https://doi.org/10.1109/MCD.1999.768560

Hou, P. X., Orikasa, H., Yamazaki, T., Matsuoka, K., Tomita, A., Setoyama, N., Fukushima, Y., & Kyotani, T. (2005). Synthesis of nitrogen-containing microporous carbon with a highly ordered structure and effect of nitrogen doping on H2O adsorption. *Chemistry of Materials*, *17*(20), 5187–5193. https://doi.org/10.1021/CM051094K

Hou, X., & Choy, K. L. (2006). Processing and Applications of Aerosol-Assisted Chemical Vapor Deposition. *Chemical Vapor Deposition*, *12*(10), 583–596. https://doi.org/10.1002/CVDE.200600033

Huang, L. Y., & Meng, L. (2007). Effects of film thickness on microstructure and electrical properties of the pyrite films. *Materials Science and Engineering: B*, *137*(1–3), 310–314. https://doi.org/10.1016/J.MSEB.2006.11.029

Kim, H., Jung, J. C., Park, D. R., Baeck, S. H., & Song, I. K. (2007). Preparation of H5PMo10V2O40 (PMo10V2) catalyst immobilized on nitrogen-containing mesoporous carbon (N-MC) and its application to the methacrolein oxidation. *Applied Catalysis A: General*, *320*, 159–165. https://doi.org/10.1016/J.APCATA.2007.01.034

Liu, A., Wu, H., Zhu, J., Han, J., & Niu, L. (2008). Evolution of compressive stress and electrical conductivity of tetrahedral amorphous carbon films with phosphorus incorporation. *Diamond and Related Materials*, *17*(11), 1927–1932. https://doi.org/10.1016/J.DIAMOND.2008.04.008

Miyajima, Y., Nitta, S., Silva, S. R. P., & Zeze, D. A. (2005). Surface induced bulk modifications of amorphous carbon nitride films by post-deposition oxygen and hydrogen plasma treatment. *Thin Solid Films*, *491*(1–2), 161–167. https://doi.org/10.1016/J.TSF.2005.06.033

Mominuzzaman, S. M., Rusop, M., Soga, T., Jimbo, T., & Umeno, M. (2006). Nitrogen doping in camphoric carbon films and its application to photovoltaic cell. *Solar Energy Materials and Solar Cells*, *90*(18–19), 3238–3243. https://doi.org/10.1016/J.SOLMAT.2006.06.037

Nitta, S., Aono, M., Katsuno, T., & Naruse, Y. (2003). Amorphous carbon nitride deposition by nitrogen radical sputtering C+N+O+H. *Diamond and Related Materials*, *12*(2), 219–226. https://doi.org/10.1016/S0925-9635(03)00073-6

Park, Y. S., & Hong, B. (2008). Characteristics of sputtered amorphous carbon films prepared by a closed-field unbalanced magnetron sputtering method. *Journal of Non-Crystalline Solids*, *354*(52–54), 5504–5508. https://doi.org/10.1016/J.JNONCRYSOL.2008.08.007

Podder, J., Rusop, M., Soga, T., & Jimbo, T. (2005). Boron doped amorphous carbon thin films grown by r.f. PECVD under different partial pressure. *Diamond and Related Materials*, *14*(11–12), 1799–1804. https://doi.org/10.1016/J.DIAMOND.2005.07.020

Pradhan, D., & Sharon, M. (2007). Opto-electrical properties of amorphous carbon thin film deposited from natural precursor camphor. *Applied Surface Science*, *253*(17), 7004–7010. https://doi.org/10.1016/J.APSUSC.2007.02.030

Rusop, M., Adhikari, S., Omer, A. M. M., Soga, T., Jimbo, T., & Umeno, M. (2006). Effects of methane gas flow rate on the optoelectrical properties of nitrogenated carbon thin films

grown by surface wave microwave plasma chemical vapor deposition. *Diamond and Related Materials*, *15*(2–3), 371–377. https://doi.org/10.1016/J.DIAMOND.2005.07.034

Tan, M., Zhu, J., Han, J., Gao, W., Liu, A., & Han, X. (2008). Raman characterization of boron doped tetrahedral amorphous carbon films. *Materials Research Bulletin*, *43*(2), 453–462. https://doi.org/10.1016/J.MATERRESBULL.2007.02.037

Valentini, L., Kenny, J. M., Carlotti, G., Guerrieri, M., Signorelli, G., Lozzi, L., & Santucci, S. (2001). Effect of nitrogen addition on the elastic and structural properties of amorphous carbon thin films. *Thin Solid Films*, *389*(1–2), 315–320. https://doi.org/10.1016/S0040-6090(01)00879-3

Yang, Z., Xia, Y., Sun, X., & Mokaya, R. (2006). Preparation and hydrogen storage properties of zeolite-templated carbon materials nanocast via chemical vapor deposition: Effect of the zeolite template and nitrogen doping. *Journal of Physical Chemistry B*, *110*(37), 18424–18431. https://doi.org/10.1021/JP0639849/SUPPL_FILE/JP0639849SI20060807_100613.PDF

Zhu, H., Wei, J., Wang, K., & Wu, D. (2009). Applications of carbon materials in photovoltaic solar cells. *Solar Energy Materials and Solar Cells*, *93*(9), 1461–1470. https://doi.org/10.1016/J.SOLMAT.2009.04.006